Momentum-selective metal-insulator transition in the two-dimensional Hubbard model: An 8-site dynamical cluster approximation study

Philipp Werner,[1] Emanuel Gull,[2] Olivier Parcollet,[3] and Andrew J. Millis[2]
[1]*Theoretische Physik, ETH Zurich, 8093 Zürich, Switzerland*
[2]*Department of Physics, Columbia University, 538 West, 120th Street, New York, New York 10027, USA*
[3]*Institut de Physique Théorique, CEA, IPhT, CNRS, URA 2306, F-91191 Gif-sur-Yvette, France*
(Received 24 June 2009; published 24 July 2009)

Metal-insulator transitions in the paramagnetic phase of the two-dimensional square-lattice Hubbard model are studied using the dynamical cluster approximation with eight momentum cells. We show that both the interaction-driven and the doping-driven transitions are multistage and momentum-sector specific with Fermi-liquid metal and fully gapped insulator phases separated by an intermediate phase, in which some regions of the Brillouin zone are gapped while others sustain gapless quasiparticles. We argue that this is the coarse-grained version of a gradually shrinking arc or pocket. A pronounced particle-hole asymmetry is found.

DOI: 10.1103/PhysRevB.80.045120 PACS number(s): 71.10.Fd, 71.27.+a, 71.30.+h, 74.72.−h

I. INTRODUCTION

The metal-insulator transition in strongly interacting Fermion systems is one of the central issues in condensed-matter physics.[1] The transition observed in the high-T_c cuprate family of materials is particularly interesting. As the doping δ (here defined as the difference of carrier concentration from 1 carrier per CuO_2 unit) is reduced to zero, the materials become less metallic with an insulating phase occurring at zero doping. Experiments, including analyses of the temperature dependence of the London penetration depth,[2,3] normal-state[4] and superconducting[5,6] Raman spectra, c-axis conductivities,[7] and photoemission[8] and scanning tunneling microscopy[9] (for a review see Ref. 10) suggest that the transition is driven by a doping-dependent decrease in the size of the region of momentum space which can support well-defined mobile quasiparticles. Understanding this behavior has proven theoretically challenging. Weak-coupling renormalization-group calculations[11,12] indicate a parameter regime in which interactions involving electrons near the $(\pm\pi/2, \pm\pi/2)$ points flow to weak coupling while interactions important for electrons near the $(\pi,0)$ and $(0,\pi)$ portions of the Fermi surface flow to strong coupling for reasons attributed to antiferromagnetism[11] or Mott physics.[12] However, the basic result is a flow to a strong-coupling regime where the equations no longer apply and the physics must be studied by other methods.

Dynamical mean-field theory (DMFT) (Refs. 13 and 14) has provided valuable insights into the physics of strongly correlated materials. Its original single-site version averages physical quantities over the entire Brillouin zone. Kusunose[15] has used single-site dynamical mean-field theory to obtain an estimate of the irreducible vertex which is then used in a Bethe-Saltpeter equation to obtain the self energy. Cluster extensions of DMFT provide direct measurements albeit with limited momentum resolution[16–20] and have indicated interesting momentum-dependent behavior.[21–30] However, most of the works were based on studies of two- and four-site clusters where the momentum resolution is so coarse that information about variation around the Fermi surface must be inferred from averages involving momentum regions far from the Fermi surface. Important exceptions are the work of Macridin *et al.*[31] and Vidhyadhiraja *et al.*[32] who studied 16-site clusters, identifying a pseudogap phase at doping 0.05[31] and a critical point defined in terms of a change of behavior in the self energy.[32] We comment on the relation of our results to these works in the conclusion.

In this paper, we use a recently developed continuous-time auxiliary field quantum Monte Carlo algorithm[33] to perform direct computations of the change in the electron spectral function and self energy around the Fermi surface. We study the 8-site cluster shown in Fig. 1 and examine a range of interaction strengths and carrier concentrations. An attractive feature of this cluster is that the Fermi surface of the noninteracting problem (shown as the heavy line) passes through two symmetry-independent sectors (labeled B and C), so that a coarse-grained approximation to the variation around the Fermi surface can be studied directly.

Our principal finding is a two-stage metal-insulator transition in both the interaction-driven and doping-driven cases: the Fermi-liquid metal and fully gapped insulator are separated by an intermediate phase, shown as the hashed region in the right panel of Fig. 1, in which sector C is gapped while sector B remains gapless. The metal-insulator transition is a

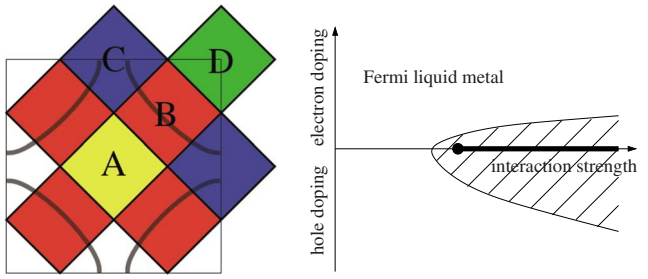

FIG. 1. (Color online) Left panel: Brillouin zone partitioning associated with the 8-site cluster and definition of the four inequivalent momentum sectors A, B, C, and D. The noninteracting Fermi surface for $t'=-0.15t$ and density $n=1$ is indicated by the gray line. Right panel: sketch of the paramagnetic-state DCA phase diagram of the Hubbard model on this cluster showing a Fermi-liquid metal phase, an intermediate phase (hashed region), and the insulating state (heavy horizontal line).

momentum-selective transition of the kind discussed by Ferrero *et al.* in Ref. 28.

II. MODEL AND METHOD

The one-band Hubbard model in two dimensions reads

$$H = \sum_{p,\sigma} \epsilon_p c^\dagger_{p,\sigma} c_{p,\sigma} + U \sum_i n_{i,\uparrow} n_{i,\downarrow}, \tag{1}$$

with $\epsilon_p = -2t(\cos(p_x)+\cos(p_y)) - 4t' \cos(p_x)\cos(p_y)$ denoting the electron dispersion and U the on-site repulsion. We are interested in the low-temperature behavior as a function of interaction strength U and doping δ. We use the dynamical cluster approximation (DCA) formulation of multisite dynamical mean-field theory,[16,20] in which the Brillouin zone is divided into $N=8$ "patches" defined by the basis functions $\phi_\alpha(p)$, which are 1 for p in patch α and zero otherwise (see Fig. 1). The momentum dependence of the self energy becomes $\Sigma(p,\omega) \to \Sigma_{\alpha=1}^{8} \phi_\alpha(p) \Sigma_\alpha(\omega)$ and the frequency-dependent functions $\Sigma_\alpha(\omega)$, $\alpha = 1, \ldots, 8$ are obtained from the solution of an appropriately defined 8-site quantum impurity model.[20] We solve the impurity model with the continuous-time auxiliary-field technique[33] with delayed updates.[34] Results are presented for $t'=0$ (where the less severe sign problem allows us to access lower temperatures) and $t'=-0.15t$, which is computationally accessible but more "generic" than $t'=0$ because the electron-hole symmetry is broken and the van Hove singularity is removed from the half-filled Fermi surface. The lowest temperature accessible with the computational resources available to us is $\beta t \approx 40$ at $U < 8t$ corresponding (with the conventional high-T_c band parametrization[35]) to ~ 100 K.

III. RESULTS

A. Interaction-driven transition

We probe the transition via the sector-specific impurity-model Green functions evaluated at the midpoint $\beta/2$ of the imaginary time interval. This quantity is directly measured in our simulations and is related to the value of the spectral function of the α sector $A_\alpha(\omega)$ near the Fermi level ($\omega=0$) by

$$\beta G_\alpha(\beta/2) = -\int \frac{dy}{\cosh(y)} A_\alpha(2y/\beta). \tag{2}$$

Figure 2 shows our results for the sectors (B and C) which contain the Fermi surface at half filling. In sector B (open symbols) we see for $U \lesssim 6.3t$ a weakly temperature-dependent value which is consistent with the noninteracting Fermi-surface density of states at density $n=1$. For $U \gtrsim 6.5t$ the density of states is very small indicating a gapped state. The noninteracting density of states in sector C (full symbols) is larger and more strongly temperature dependent due to the van Hove singularity, which at $t'=0$ is at the half-filled Fermi level and at $t'=-0.15t$ is about $0.2t$ below. We see that the temperature dependence changes sign at $U \approx 5.5t$ ($t'=0$) and $U \approx 5.8t$ ($t'=-0.15t$); for larger U the evolution is toward an insulating state. Thus sector C undergoes a gap-opening transition at a smaller U than sector B, both for t'

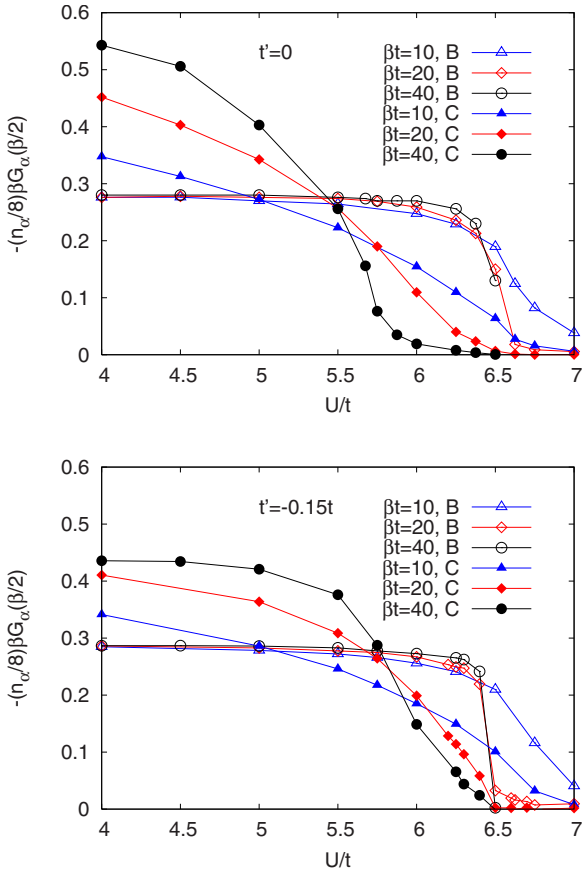

FIG. 2. (Color online) Sector B (open symbols) and C (filled symbols) Green functions, scaled by the number of equivalent sectors n_α and evaluated at the midpoint of the imaginary time interval as a function of U at half filling. The top panel shows results for $t'=0$; the bottom panel for $t'=-0.15t$.

$=0$ and $t'=-0.15t$. We emphasize that this two-stage transition is directly visible in our data and is a result enabled by the momentum resolution of the 8-site cluster. It is different from the result of single-site DMFT, which predicts a single transition at a large $U \sim 1.5W$ with W (here $8t$) the full bandwidth and from the result of four-site cluster calculations, which predict a single transition at $U \sim 4.2t$ (Ref. 27) or $U \sim 5.5t$ (Ref. 26). The difference in critical U arises from the use of the dynamical cluster approximation in Ref. 27 and cellular dynamical mean field theory in Ref. 26.

Figure 3 displays the imaginary part of the Matsubara axis self energy in sectors B and C for several U in a range containing the two transitions. We present results obtained for $t'=0$ both because the absence of the sign problem allows us to obtain more accurate data and because the particle-hole symmetry implies Re $\Sigma=0$ which simplifies the discussion, but our results for $t'=-0.15t$ are consistent. The smaller U curves of Fig. 3 show the low-frequency behavior expected in a Fermi-liquid phase Im $\Sigma(i\omega_n) \sim -\omega_n(Z^{-1}-1)$ with quasiparticle residue Z decreasing as U is increased toward the transition. The larger U curves reveal the low-frequency behavior Im $\Sigma(i\omega_n) \sim -\Delta^2/\omega_n$ expected in an insulating phase with Δ decreasing as U is decreased toward the metal-insulator transition value. In the intermediate regime $5.5 \lesssim U/t \lesssim 6$, Σ_C exhibits an insulating behavior while

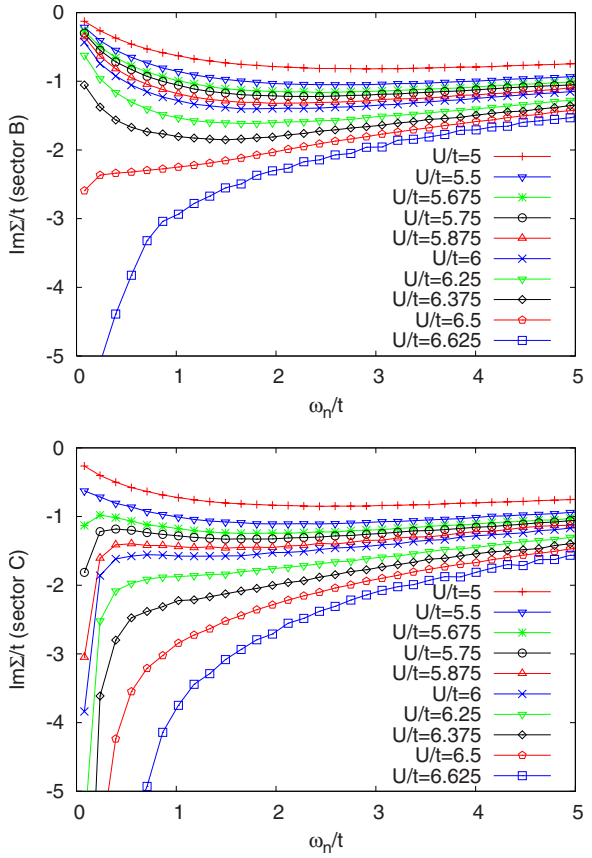

FIG. 3. (Color online) Imaginary part of the self energy in momentum sectors B and C for half filling and $t'=0$ ($\beta t=40$). The interaction strengths are (from top to bottom) $U/t=5$, 5.5, 5.675, 5.75, 5.875, 6, 6.25, 6.375, 6.5, and 6.625.

Σ_B appears consistent with the Fermi-liquid expectation.

B. Doping-driven transition

Figures 4 and 5 present the doping-driven transitions for $U=7t$, large enough that at half filling all sectors are gapped. We denote by μ the chemical potential minus the Hartree shift $Un/2$. In the particle-hole symmetric case ($t'=0$, Fig. 4) we plot the total number of electrons doped into sectors B and C for several temperatures. At the lowest temperature, $\beta t=40$, the system remains half filled up to $\mu\approx 0.5t$, consistent with the presence of a gap in the spectral function. Increasing the chemical potential further induces a metal-insulator transition but all the dopants initially go into the B sector. Only at a substantially larger chemical potential ($\mu\approx t$) does the C sector become metallic and at this point the total doping has already reached $\delta\approx 0.04$. For $t'=-0.15t$, hole-doping leads to a wide range of chemical potentials where sector C remains insulating while sector B is doped. On the electron-doped side, the two transitions occur almost simultaneously and the onset of doping in sector B appears very sudden. However, the inset to Fig. 5 shows that even on the electron-doped side there is a small window of chemical potential ($\mu\sim 0.7t$) where sector C develops a gap but sector B remains gapless.

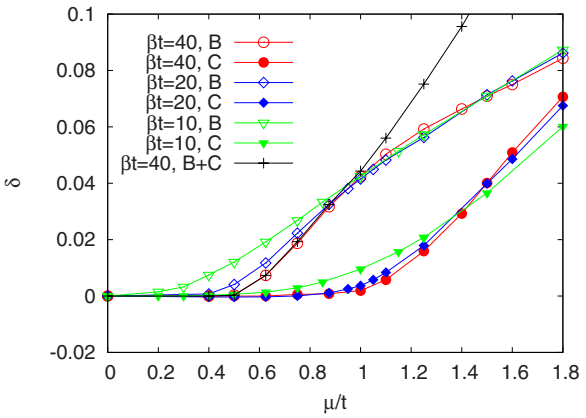

FIG. 4. (Color online) B- and C-sector dopings (summed over spin and sector degeneracy) as a function of chemical potential for $U/t=7$, $t'=0$ at $\beta t=10$, 20, and 40. The doping-driven transition is sector selective with dopants appearing first in the B-sector.

The particle-hole asymmetry in the model with $t'=-0.15t$ is evident also in the self energies. We find that on the electron-doped side, at high dopings $\delta\gtrsim 0.15$ the two sectors have the same quasiparticle residue ($Z_\alpha\approx 0.5$ for $\delta=0.23$); as doping is decreased, Z decreases in both sectors but at a slightly faster rate in sector C. Down to a doping of $\delta\approx 0.08$, Z is reasonably well defined in both sectors, is larger than 0.2, and is only weakly anisotropic. For lower dopings in the vicinity of the C-sector gapping the behavior is not Fermi-liquid-like and the C-sector self energy becomes much larger. Figure 6 shows that the hole-doped side exhibits a richer behavior. An analysis of the real and imaginary parts of $1/\Sigma$ (not shown) reveals that at $-0.4t<\mu$, where the model is insulating (gaps in all sectors), the low-frequency self energy is dominated by a pole $\Sigma_\alpha\sim\Delta_\alpha^2/(i\omega_n-\omega_p^\alpha)$ with pole strengths $\Delta_B/t\approx 3$ and $\Delta_C/t\approx 5$ and position ω_p^α shifting with chemical potential. This shift is responsible for the changes evident in the three undoped traces. In the sector-

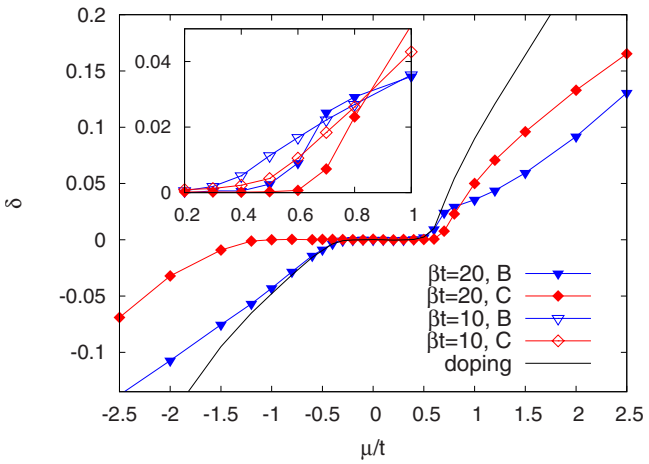

FIG. 5. (Color online) Main panel: B- and C-sector dopings (summed over spin and sector degeneracy) and total doping as a function of chemical potential for $U/t=7$, $t'=-0.15t$ at $\beta t=20$. Inset: expansion of the electron-doped metal-insulator transition region showing the temperature dependence.

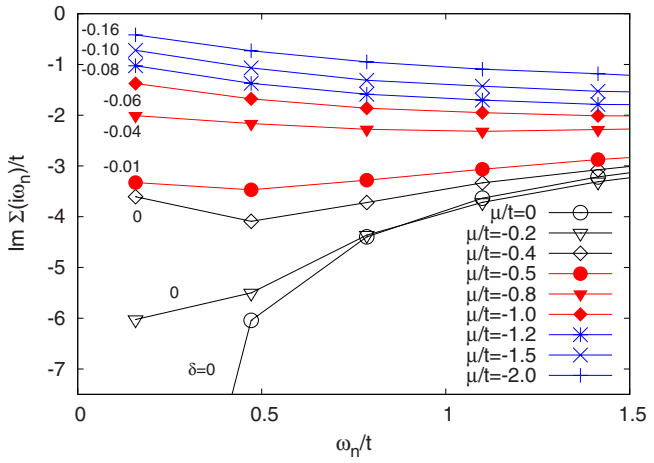

FIG. 6. (Color online) Imaginary part of B-sector self energies for the doped Hubbard model at $U=7t$, $t'=-0.15t$, and $\beta t=20$. Traces indicated by open circles, triangles, and diamonds correspond to μ where both sector B and sector C are gapped; traces marked by full circles, triangles, and diamonds correspond to μ where sector C remains undoped and sector B is doped, while traces marked by asterisks, crosses, and plus signs correspond to μ where both sectors are doped.

selective regime where B is doped and C is not, the B self energy is that of a "bad metal" ($\lim_{\omega_n\to 0} \mathrm{Im}\,\Sigma(i\omega_n)\neq 0$): any Fermi-liquid coherence scale would be far below the temperature regime we can access. One possibility is that this behavior corresponds to a momentum average of a "nodal-metal" state in which the density of states vanishes except at one gapless point. It could also indicate the appearance of arcs or pockets. Higher momentum resolution would be required to resolve this issue. In any event, as the doping is increased into the regime where all sectors are ungapped the self energy evolves toward Fermi-liquid behavior (with $Z_\alpha \approx 0.4$ for $\delta=-0.23$). The self-energy transition studied in Ref. 32 can be seen as a change from $\mathrm{Im}\,\Sigma(i\omega_n)\sim\omega_n$ to a more flat ω_n dependence as δ drops below ~ 0.15. This change occurs well before the C-sector gapping transition ($\delta\sim 0.08$).

IV. DISCUSSION

One can view the differentiation between sectors B and C as an orbitally selective transition of the effective impurity model.[28] While orbitally selective transitions may be destabilized by a Kondo coupling to other sectors, the gapped sector C is twofold degenerate and we believe that the two electrons in this sector are antiferromagnetically coupled (or form singlets). In this case, the sector-selective state is stable against a Kondo coupling and the effect should survive beyond the DCA approximation. On physical grounds it seems plausible that the sector-selective transition is the expression, within our coarse momentum resolution, of a continuous reduction in Fermi-surface area. Preliminary results for a 16-site cluster with Fermi surface crossing four inequivalent sectors indicate a four-stage metal-insulator transition consistent with the gradual opening of a gap near $(0,\pi)$.

The results are intriguingly similar to data on high-T_c materials where a growing body of evidence indicates that in the hole-doped materials the metal-insulator transition occurs by a reduction in the size of the k-space regions which can support mobile particles, while the electron-doped materials behave more conventionally (apart from the effects of long-ranged commensurate density wave order not included here). In our calculation the important factor underlying the asymmetry is the distance of the van Hove singularity from the chemical potential. On the electron-doped side the sector-selective region shrinks with increasing particle-hole asymmetry and completely vanishes for $t'=-0.3t$.

Our finding, of a "pseudogap" more pronounced for hole-doped than for electron-doped materials, is consistent with previous work comparing $\pm 5\%$ doping[24,31] but our improved temperature resolution and our examination of a range of interaction strengths and dopings enables us to identify the origin of the pseudogap as a sector-selective transition. We note, though, that while Ref. 31 reported a large density of states near $(0,\pi)$ at 5% doping both for $t'=0$ and $t'=-0.3t$ on a cluster with 16 sites, we find (for $t'=0$ and $t'=-0.15t$ on an 8-site cluster) that for both electron and hole doping, carriers first appear near the *nodes* (sector B) with sector C remaining gapped. However, after the initial doping, the sector C occupancy increases rapidly, so the difference may be a doping-level effect.

Our results differ in some aspects with those reported by Kusunose,[15] who studied a model with $t'=0$ and $U=8t$ and found at half filling a quasiparticle band with a small weakly momentum-dependent pseudogap. By contrast, at this value of the interaction strength we find that the half-filled model is characterized by a large gap (varying somewhat around the Fermi surface) and no in-gap quasiparticle band.

The precise physical state which is represented in the DCA calculations by the sector-selective transition remains to be resolved. One theoretical possibility is a "Fermi arc," another is a "hole pocket" as might arise from antiferromagnetic correlations or order. While different periodization/interpolation/broadening schemes favor one result or the other (see e.g., Fig. 4 of Ref. 30), distinguishing these requires a much finer momentum resolution than is presently available. Here we simply note that if we assume that when sector B is metallic and C is not, we have a hole pocket centered at $(\pi/2,\pi/2)$ which is elliptical with major axis $2r_1$ and minor axis $2r_2$, it is possible to estimate the aspect ratio r_2/r_1 from the doping [$\delta\approx 0.04$ for $t'=0$ (Fig. 4) and $\delta\approx 0.08$ for $t'=-0.15t$ (Fig. 5)] at which the sector C metal-insulator transition occurs (assuming that this is the point where the ellipse enters sector C). This calculation yields an aspect ratio of about 10:1 for $t'=0$ and about 5:1 for $t'=-0.15t$, roughly consistent with the very anisotropic hole pockets observed in mean-field calculations.[36,37]

V. CONCLUSIONS

Previous cluster DMFT work indicated a pseudogap phenomenon more pronounced for hole-doped than electron-doped materials. Our improved momentum resolution confirms that the effects inferred from two- and four-site

calculations[21–27] indeed reflect behavior associated with near-Fermi-surface states, while the improved temperature resolution and the examination of a range of interactions and dopings reveals that the pseudogap observed in Ref. 31 is caused by a momentum-selective transition.

On the other hand, the quantum phase transition reported in Ref. 32 is marked by the appearance of a non-Fermi-liquid self energy. Figure 6 and the corresponding data for sector C (not shown) indicate that this phenomenon is visible in our results as a change from $\mathrm{Im}\,\Sigma(i\omega_n) \sim \omega_n$ to a flatter ω_n dependence as δ drops below ~ 0.15 ($t' = -0.15t$). This change in behavior, therefore, occurs well before the sector-C gapping transition ($\delta \sim 0.08$) and appears to have a different origin.

The important open questions concern the physical origin of the gapping behavior. We find cluster antiferromagnetic correlations which are large and grow rapidly in the vicinity of the metal-insulator transitions. However, in the model with $t' = -0.15t$, the correlation functions do not change dramatically across the sector-selective transitions suggesting that the phenomenon may not be antiferromagnetically driven, which would support the interpretation of Läuchli *et al.* in Ref. 12. Optimized implementations of the hybridization-expansion technique[38] should permit examination of the cluster eigenstates along the lines of Ref. 27 and thus provide direct information on the role of singlet formation and antiferromagnetism.

ACKNOWLEDGMENTS

We thank A. Lichtenstein and T. M. Rice for helpful conversations and acknowledge support from NSF under Grant No. DMR-0797074 (A.J.M., partial support E.G. and P.W.), the Swiss National Science Foundation (Grant No. PP002-118866), and the ANR under Grant ECCE. The calculations were done on the Brutus cluster at ETH Zurich using a code based on ALPS.[39]

[1] M. Imada, A. Fujimori, and Y. Tokura, Rev. Mod. Phys. **70**, 1039 (1998).
[2] P. A. Lee and X. G. Wen, Phys. Rev. Lett. **78**, 4111 (1997).
[3] A. J. Millis, S. M. Girvin, L. B. Ioffe, and A. I. Larkin, J. Phys. Chem. Solids **59**, 1742 (1998).
[4] M. Le Tacon, A. Sacuto, and D. Colson, Phys. Rev. B **71**, 100504(R) (2005).
[5] M. Le Tacon, A. Sacuto, A. Georges, G. Kotliar, Y. Gallais, D. Colson, and A. Forget, Nat. Phys. **2**, 537 (2006).
[6] W. Guyard, M. Le Tacon, M. Cazayous, A. Sacuto, A. Georges, D. Colson, and A. Forget, Phys. Rev. B **77**, 024524 (2008).
[7] L. B. Ioffe and A. J. Millis, Phys. Rev. B **58**, 11631 (1998).
[8] M. Shi, A. Bendounan, E. Razzoli, S. Rosenkranz, M. R. Norman, J. C. Campuzano, J. Chang, M. Mansson, Y. Sassa, T. Claesson, O. Tjernberg, L. Patthey, N. Momono, M. Oda, M. Ido, S. Guerrero, C. Mudry, and J. Mesot, arXiv:0810.0292 (unpublished).
[9] Y. Kohsaka, C. Taylor, P. Wahl, A. Schmidt, J. Lee, K. Fujita, J. W. Alldredge, K. McElroy, J. Lee, H. Eisaki, S. Uchida, D.-H. Lee, and J. C. Davis, Nature (London) **454**, 1072 (2008).
[10] S. Hüfner, M. A. Hossain, A. Damascelli, and G. A. Sawatzky, Rep. Prog. Phys. **71**, 062501 (2008).
[11] D. Zanchi and H. Schulz, Europhys. Lett. **44**, 235 (1998).
[12] A. Läuchli, C. Honerkamp, and T. M. Rice, Phys. Rev. Lett. **92**, 037006 (2004).
[13] A. Georges, G. Kotliar, W. Krauth, and M. J. Rozenberg, Rev. Mod. Phys. **68**, 13 (1996).
[14] G. Kotliar, S. Y. Savrasov, K. Haule, V. S. Oudovenko, O. Parcollet, and C. A. Marianetti, Rev. Mod. Phys. **78**, 865 (2006).
[15] H. Kusunose, J. Phys. Soc. Jpn. **75**, 054713 (2006).
[16] M. H. Hettler, A. N. Tahvildar-Zadeh, M. Jarrell, T. Pruschke, and H. R. Krishnamurthy, Phys. Rev. B **58**, R7475 (1998).
[17] A. I. Lichtenstein and M. I. Katsnelson, Phys. Rev. B **62**, R9283 (2000).
[18] G. Kotliar, S. Y. Savrasov, G. Pálsson, and G. Biroli, Phys. Rev. Lett. **87**, 186401 (2001).
[19] S. Okamoto, A. J. Millis, H. Monien, and A. Fuhrmann, Phys. Rev. B **68**, 195121 (2003).
[20] Th. Maier, M. Jarrell, Th. Pruschke, and M. H. Hettler, Rev. Mod. Phys. **77**, 1027 (2005).
[21] M. Civelli, M. Capone, S. S. Kancharla, O. Parcollet, and G. Kotliar, Phys. Rev. Lett. **95**, 106402 (2005).
[22] O. Parcollet, G. Biroli, and G. Kotliar, Phys. Rev. Lett. **92**, 226402 (2004).
[23] K. Haule and G. Kotliar, Phys. Rev. B **76**, 104509 (2007).
[24] B. Kyung, S. S. Kancharla, D. Sénéchal, A.-M. S. Tremblay, M. Civelli, and G. Kotliar, Phys. Rev. B **73**, 165114 (2006).
[25] S. Chakraborty, D. Galanakis, and P. Phillips, Phys. Rev. B **78**, 212504 (2008).
[26] H. Park, K. Haule, and G. Kotliar, Phys. Rev. Lett. **101**, 186403 (2008).
[27] E. Gull, P. Werner, M. Troyer, and A. J. Millis, EPL **84**, 37009 (2008).
[28] M. Ferrero, P. S. Cornaglia, L. De Leo, O. Parcollet, G. Kotliar, and A. Georges, EPL **85**, 57009 (2009).
[29] T. D. Stanescu and G. Kotliar, Phys. Rev. B **74**, 125110 (2006).
[30] S. Sakai, Y. Motome, and M. Imada, Phys. Rev. Lett. **102**, 056404 (2009).
[31] A. Macridin, M. Jarrell, T. Maier, P. R. C. Kent, and E. D'Azevedo, Phys. Rev. Lett. **97**, 036401 (2006).
[32] N. S. Vidhyadhiraja, A. Macridin, C. Sen, M. Jarrell, and M. Ma, Phys. Rev. Lett. **102**, 206407 (2009).
[33] E. Gull, P. Werner, O. Parcollet, and M. Troyer, EPL **82**, 57003 (2008).
[34] G. Alvarez, M. S. Summers, D. E. Maxwell, M. Eisenbach, J. S. Meredith, J. M. Larkin, J. Levesque, T. A. Maier, P. R. C. Kent, E. F. D'Azevedo, and T. C. Schulthess, in *SC '08: Proceedings of the 2008 ACM/IEEE Conference on Supercomputing*, Austin, 2008 (IEEE Press, Piscataway, NJ, 2008), pp. 1–10.
[35] O. K. Andersen, A. I. Liechtenstein, O. Jepsen, and F. Paulsen, J. Phys. Chem. Solids **56**, 1573 (1995).

[36] B. I. Shraiman and E. D. Siggia, Phys. Rev. Lett. **61**, 467 (1988).
[37] C. L. Kane, P. A. Lee, and N. Read, Phys. Rev. B **39**, 6880 (1989).
[38] P. Werner, A. Comanac, L. de Medici, M. Troyer, and A. J. Millis, Phys. Rev. Lett. **97**, 076405 (2006).
[39] A. F. Albuquerque, F. Alet, P. Corboz, *et al.*, J. Magn. Magn. Mater. **310**, 1187 (2007).